

REPORT DOCUMENTATION PAGE

Form Approved
OMB NO. 0704-0188

Public Reporting burden for this collection of information is estimated to average 1 hour per response, including the time for reviewing instructions, searching existing data sources, gathering and maintaining the data needed, and completing and reviewing the collection of information. Send comment regarding this burden estimates or any other aspect of this collection of information, including suggestions for reducing this burden, to Washington Headquarters Services, Directorate for Information Operations and Reports, 1215 Jefferson Davis Highway, Suite 1204, Arlington, VA 22202-4302, and to the Office of Management and Budget, Paperwork Reduction Project (0704-0188,) Washington, DC 20503.

1. AGENCY USE ONLY (Leave Blank)		2. REPORT DATE 01/14/2003	3. REPORT TYPE AND DATES COVERED Final Technical Report 01/Jul/98 - 30/Jun/02	
4. TITLE AND SUBTITLE Fundamental optical criteria to optimize tunable solid state laser crystals			5. FUNDING NUMBERS DAAG55-98-1-0397	
6. AUTHOR(S) P.I. : R. R. Alfano Researchers: M. Yu. Sharonov, S.Owen, W.B. Wang				
7. PERFORMING ORGANIZATION NAME(S) AND ADDRESS(ES) City College of New York Convent Avenue and 138th Street New York, NY 10031			8. PERFORMING ORGANIZATION REPORT NUMBER 070401	
9. SPONSORING / MONITORING AGENCY NAME(S) AND ADDRESS(ES) U. S. Army Research Office P.O. Box 12211 Research Triangle Park, NC 27709-2211			10. SPONSORING / MONITORING AGENCY REPORT NUMBER 37569.1-PH	
11. SUPPLEMENTARY NOTES The views, opinions and/or findings contained in this report are those of the author(s) and should not be construed as an official Department of the Army position, policy or decision, unless so designated by other documentation.				
12 a. DISTRIBUTION / AVAILABILITY STATEMENT Approved for public release; distribution unlimited.			12 b. DISTRIBUTION CODE	
13. ABSTRACT (Maximum 200 words) Impurity ion-doped dielectric crystals have extensive applications in lasers, photodetectors, nonlinear crystals, displays, and scintillators. The performance of these devices is intrinsically correlated with their ability to transfer energy from the photoexcited impurity ion into the surrounding host. We have experimentally shown the importance of exact energy resonance between phonon and local modes in the decay pathway route of the nonradiative relaxation processes. Resonance Raman scattering and up-converted hot luminescence measurements performed in $\text{Cr}^{4+}:\text{Ca}_2\text{GeO}_4$ have shown that there is only one phonon-local mode pair at 733 cm^{-1} whose exact energy resonance provides the decay channel during the initial steps of the nonradiative relaxation of the photoexcited impurity ion. By understanding these nonradiative decay mechanisms, we have developed criteria for laser crystals with reduced nonradiative relaxation.				
14. SUBJECT TERMS Nonradiative relaxation, hot luminescence, energy resonance, on-and-off-resonance Raman scattering, local and phonon modes			15. NUMBER OF PAGES 9	
			16. PRICE CODE	
17. SECURITY CLASSIFICATION OR REPORT UNCLASSIFIED	18. SECURITY CLASSIFICATION ON THIS PAGE UNCLASSIFIED	19. SECURITY CLASSIFICATION OF ABSTRACT UNCLASSIFIED	20. LIMITATION OF ABSTRACT UL	

NSN 7540-01-280-5500

Standard Form 298 (Rev.2-89)
Prescribed by ANSI Std. Z39-18
298-102

20030306 080

FINAL PROGRESS REPORT
For ARO Grant DAAG55-98-1-0397 (RF 47404)

Entitled "Fundamental optical criteria to optimize tunable solid state laser crystals"

Period Covered: 01/01/1999 – 06/30/2002

1. Participating Scientific Personnel:

M. Yu Sharonov, S. Owen, W. B. Wang, and R. R. Alfano

2. Report of Inventions: N/A

3. Publications:

1. S. G. Demos, Dana M. Calistru, Scot Owen, A. B. Bykov, V. Petricevic, and R. R. Alfano, "Primary decay pathway of a local mode of a photoexcited ion into a dielectric crystal host lattice"– Physical Review Letters, 82, 2556 (1999)
2. A.B. Bykov, V. Petricevic, J. Steiner, Di Yao, L. L. Isaacs, M. R. Kakta, and R.R. Alfano, "Flux growth and characterization of $\text{Cr}^{4+}:\text{Ca}_2\text{GeO}_4$ crystals as a New near infrared tunable laser material," Journal of Crystal Growth, 211, 295, (2000)
3. Bing Xu, J. M. Evans, V. Petricevic, S. P. Guo, O. Maksimov, M. C. Tamargo, and R. R. Alfano, "Continuous-wave and passively mode-locked operation of a Cunyite ($\text{Cr}^{4+}:\text{Ca}_2\text{GeO}_4$) laser," Applied Optics, 39, 4875 (2000)
4. C. H. Liu, Scot Owen, W. B. Wang, G. Zhang, A. B. Bykov, V. Petricevic, and R. R. Alfano, "Raman Scattering Study of Cunyite ($\text{Cr}^{4+}:\text{Ca}_2\text{GeO}_4$) Laser Crystals", in the Conference Program of the 2000 OSA Annual Meeting, P 83 (2000). Presented at the 2000 OSA Annual Meeting, Oct. 22-26, 2000, Providence, Rhode Island

4. Statement of the Problem Studied:

Impurity ion-doped dielectric crystals have extensive applications in lasers, photodetectors, nonlinear crystals, displays, and scintillators. The performance of these devices is intrinsically correlated with their ability to transfer energy from the photoexcited impurity ion into the surrounding host. We have experimentally shown the importance of exact energy resonance between phonon and local modes in the decay pathway route of the nonradiative relaxation processes. Resonance Raman scattering and

up-converted hot luminescence measurements performed in $\text{Cr}^{4+}:\text{Ca}_2\text{GeO}_4$ have shown that there is only one phonon-local mode pair whose exact energy resonance provides the decay channel during the initial steps of the nonradiative relaxation of the photoexcited impurity ion.

5. Scientific Progress and Accomplishment:

The interaction between the local modes (ω_L) and the phonon modes (ω_P) plays a crucial role in the nonradiative relaxation in crystals. The excess energy of the photoexcited impurity ion (above the zero phonon line of a given electronic state) is temporarily stored in excited local modes that decay by local (L) and phonon (P) modes. Four decay pathways between local and phonon modes are possible for a nonradiative process: (a) intramolecular local decay route $\omega_L \rightarrow \omega_{L1} + \omega_{L2}$; (b) intermolecular phonon decay route $\omega_L \rightarrow \omega_{P1} + \omega_{P2}$; (c) mixed local and phonon decay route $\omega_L \rightarrow \omega_L + \omega_P$; and exact resonance decay route $\omega_L \rightarrow \omega_P$ ($\omega_L \sim \omega_P$). The first three decay routes are second order processes, while the last one is a first order process. The final step of the nonradiative decay is accomplished by the interaction between the accepting modes and the phonon continuum dissipating the excess energy into the lattice, returning the system to thermal equilibrium. The temporal diagram for nonradiative processes taking place in an impurity-doped crystal is shown in fig. 1. The exact energy resonance between the phonon mode at 733 cm^{-1} and the Cr^{4+}O_4 tetrahedral breathing mode A_1 at 733 cm^{-1} was demonstrated using off- and on-resonance Raman scattering. Up-converted hot luminescence measurements identified the accepting phonon mode at 733 cm^{-1} as the only participant in the first steps of the nonradiative relaxation of Cr^{4+} ions. These results demonstrate that in an impurity doped dielectric solid material the exact energy resonance between a local and a phonon mode determines the primary participating phonon mode in the initial steps of the nonradiative relaxation process. The local and phonon mode spectrum was investigated using on- and off-resonance Stokes Raman scattering with our Photon Image Acquisition System (PIAS). The material investigated was a highly efficient tunable Cunyite ($\text{Cr}^{4+}:\text{Ca}_2\text{GeO}_4$) laser crystal, which belongs to the olivine family with lattice constants of $a = 11.4 \text{ \AA}$, $b = 6.79 \text{ \AA}$ and $c = 5.24 \text{ \AA}$. A heavily doped $3 \times 5 \times 7 \text{ mm}^3$ $\text{Cr}^{4+}:\text{Ca}_2\text{GeO}_4$ single crystal, grown by a top-seeded solution growth method and containing 0.3 Cr^{4+} at % wt. was used for on- and off- resonance Raman

Temporal diagram for nonradiative processes taking place in an impurity-doped crystal

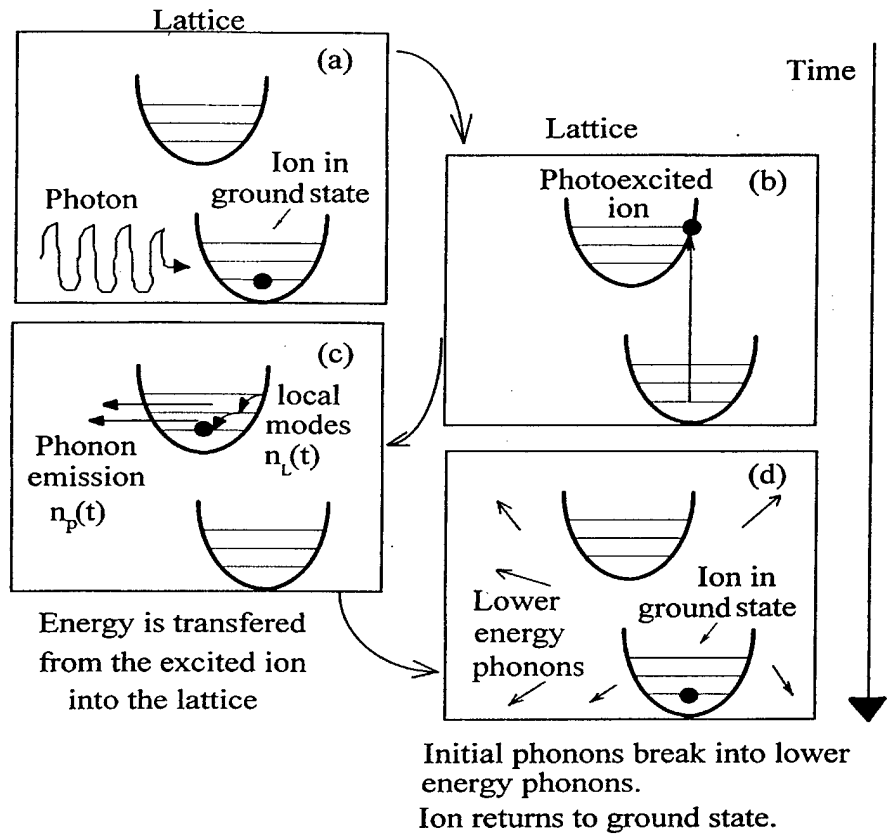


Fig. 1 Temporal diagram for nonradiative processes taking place in an impurity-doped crystal.

measurements. In addition, a $4 \times 3 \times 3 \text{ mm}^3$ undoped Ca_2GeO_4 single crystal was used for Raman measurements and allowed the identification of the phonon modes of the host.

Figure 2 shows the polarized A_g Raman spectra of $\text{Cr}^{4+}:\text{Ca}_2\text{GeO}_4$ under 632 nm (off resonance) and 621 nm (on resonance) excitations in the $550\text{-}800 \text{ cm}^{-1}$ region and the Raman spectrum of the undoped Ca_2GeO_4 crystal under 621 nm excitation. The scattering configuration was $y(\text{zz})y$ in Porto's notation. The inset in Fig. 1 shows the room temperature absorption spectrum of the sample for $E \parallel c$ axis in the $500\text{-}900 \text{ nm}$ spectral region corresponding to the ${}^3A_2 \rightarrow {}^3B_2({}^3T_1)$ dipole allowed transition. The absorption spectrum indicates that the maximum enhancement of Cr^{4+} local modes in on-resonance Raman spectra is expected under 621 nm excitation (maximum of absorption), allowing for their observation in addition to phonon modes. On the other hand, as 532 nm excitation corresponds to minimum absorption, only phonon modes are expected in the Raman spectrum of the doped sample measured under 532 nm excitation. The off-resonance Raman spectrum of $\text{Cr}^{4+}:\text{Ca}_2\text{GeO}_4$, obtained under 532 nm excitation, shows two modes located at 757 cm^{-1} and 733 cm^{-1} (see fig. 1), which are attributed to the $(\text{GeO}_4)^{4-}$ tetrahedral stretching modes ν_3 and ν_1 respectively, by analogy with the A_g Raman spectrum of Mg_2SiO_4 . The on-resonance Raman spectrum obtained under 621 nm excitation shows a marked enhancement for the 733 cm^{-1} mode only. The Raman spectrum of the undoped Ca_2GeO_4 crystal, obtained under 621 nm excitation, which contains only phonon modes, is identical to the off-resonance spectrum of the doped sample. The enhancement of the 733 cm^{-1} local modes indicates that it is the only local mode having the same energy (within spectral resolution) as the 733 cm^{-1} phonon mode. The 757 cm^{-1} phonon mode is not enhanced, as there is no local mode in resonance with it. The local mode at 733 cm^{-1} was identified as the Cr^{4+}O_4 tetrahedral stretching mode A_1 . The identification was made based on symmetry considerations and analogy with the similar local mode in $\text{Cr}^{4+}:\text{Mg}_2\text{SiO}_4$ located at 764 cm^{-1} . The space symmetry of these local modes was inferred from the scanning arrangements $y(\text{zx})y$ and $x(\text{zy})x$ and point group symmetry tables. These results clearly indicate that there is only one local mode in exact energy resonance with a phonon mode in $\text{Cr}^{4+}:\text{Ca}_2\text{GeO}_4$. Raman measurements using a spectrometer-CCD system were also performed. Figure 3 shows the Raman

RAMAN SPECTRUM OF $\text{Cr}^{4+}:\text{Ca}_2\text{GeO}_4$, $E \parallel a$ - Axis

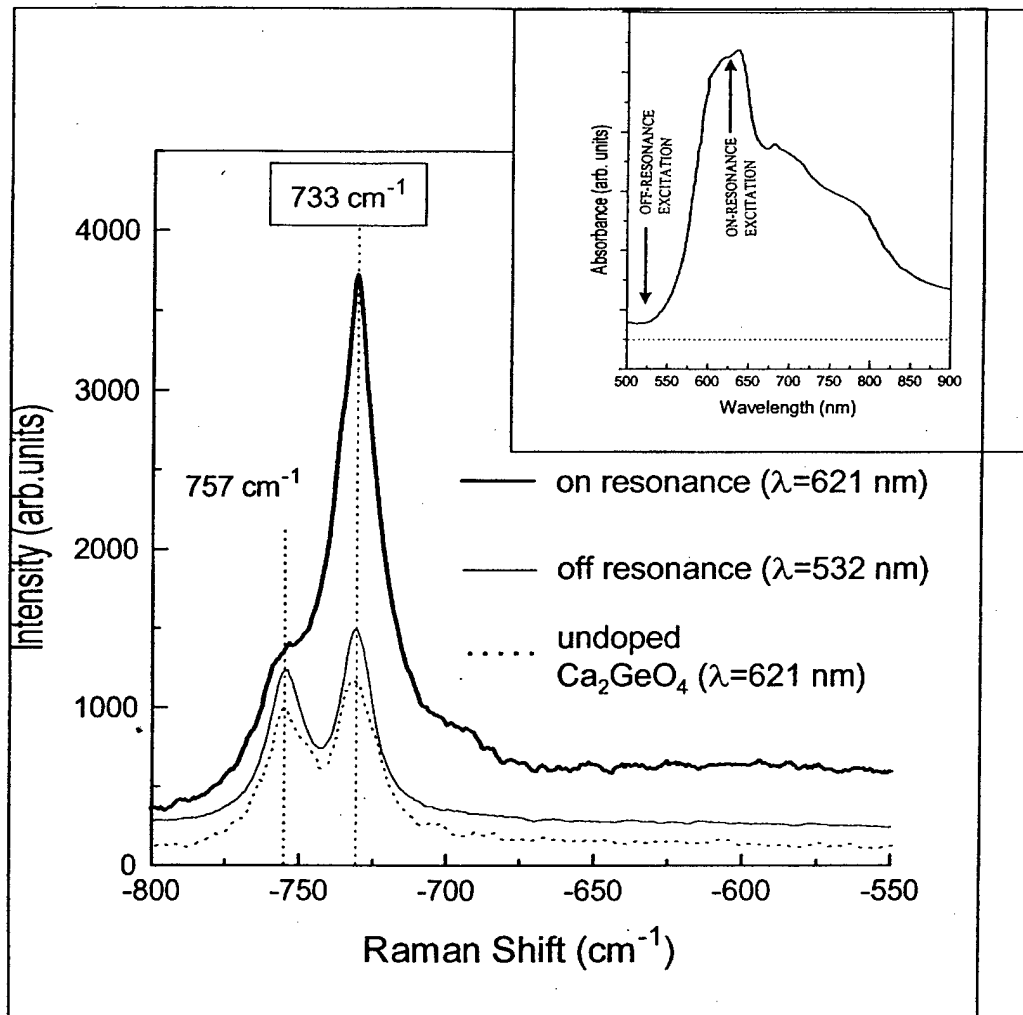


Fig. 2 Polarized resonance Raman (upper profile) and off resonance Raman (middle profile) spectra in the $550\text{-}800 \text{ cm}^{-1}$ spectral region under 621 nm and 532 nm excitation, respectively for $\text{Cr}^{4+}:\text{Ca}_2\text{GeO}_4$. The lower profile shows the Raman spectrum of the undoped Ca_2GeO_4 under 621 nm excitation. The scattering configuration is $b(cc)b$, A_g symmetry. Insert shows the polarized absorption spectrum of $\text{Cr}^{4+}:\text{Ca}_2\text{GeO}_4$ for $E \parallel c$ -axis. Spectra were obtained with the sample held at room temperature.

spectrum using 800 nm excitation in A_g symmetry, both excitation and detection polarization directions parallel to the "b" axis ($E \parallel b$). Fourteen lattice phonon modes (368 cm^{-1} , 429 cm^{-1} , 460 cm^{-1} , 671 cm^{-1} , 702 cm^{-1} , 740 cm^{-1} , 766 cm^{-1} , 1014 cm^{-1} , 1089 cm^{-1} , 1139 cm^{-1} , 1199 cm^{-1} , 1333 cm^{-1} , 1430 cm^{-1} , and 1656 cm^{-1}) were obtained from all of the polarized non-resonant Raman spectra of the undoped Ca_2GeO_4 crystal in the wider spectral region of $300\text{-}2100 \text{ cm}^{-1}$. Five Cr^{4+} impurity local modes (521 cm^{-1} , 553 cm^{-1} , 740 cm^{-1} , 971 cm^{-1} , and 1038 cm^{-1}) were obtained from all of the polarized on-resonance Raman measurements of the Cr^{4+} -doped Ca_2GeO_4 crystals. Figure 4 shows the on-resonance Raman spectrum obtained under 633 nm excitation in the $E \parallel a$ direction, where there is a marked enhancement for the $\sim 740 \text{ cm}^{-1}$ mode. The enhancement of the $\sim 740 \text{ cm}^{-1}$ mode indicates the presence of a local mode having the same energy as the $\sim 740 \text{ cm}^{-1}$ phonon mode. The other four Cr^{4+} impurity local modes do not coincide in energy with any lattice modes. Our results show that there is only one local mode ($\sim 740 \text{ cm}^{-1}$) in exact energy resonance with a phonon mode in $\text{Cr}^{4+}:\text{Ca}_2\text{GeO}_4$ crystals.

The up-converted hot luminescence spectroscopic technique utilizes a two-step excitation process. The first step photoexcites the impurity ions to an upper electronic state situated above the metastable level. In the second step, the photoexcited ions relax to the bottom of the metastable level, absorb another photon, and reach an excitation level of energy (E_{EL}) given by $E_{EL} = E_{\text{photon}} + E_{ML}$, where E_{photon} is the energy of the absorbed photon, and E_{ML} is the energy of the metastable level. Subsequent to the two step photoexcitation, radiative and nonradiative relaxation occurs and impurity ion local modes are populated. Emission arising from radiative transitions from short-lived local modes to the ground electronic state via energy transfer to select phonon modes provides information about the energy of these "active" phonons.

The energy separation between successive peaks in the up-converted hot luminescence spectra reveals the initial "steps" in the nonradiative energy transfer from the impurity ion into the lattice allowing for identification of the participating phonon modes. In $\text{Cr}^{4+}:\text{Ca}_2\text{GeO}_4$, the zero phonon peak of the near-IR emission shows that the metastable level is located at $E_{ML}=1.043 \text{ eV}$ (1189 nm). Photoexcited ions at the metastable level

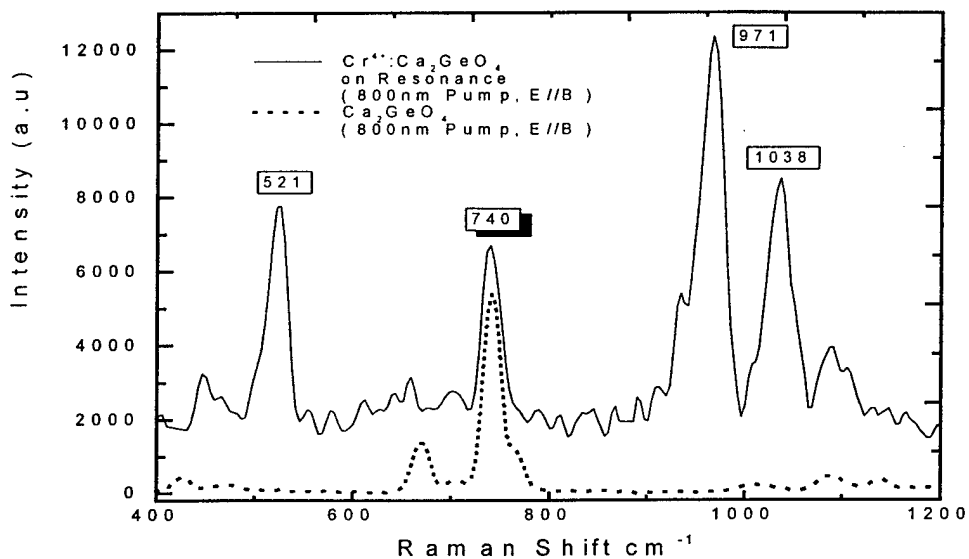


Fig.3 Resonance Raman spectrum (solid line) for doped Cr⁴⁺:Ca₂GeO₄ crystal and non-resonance Raman spectrum for undoped Ca₂GeO₄ crystal (dot line) in 400–1200 cm⁻¹ with 800 nm pump, and both excitation and detection polarization directions parallel to the “b” axis (E || b).

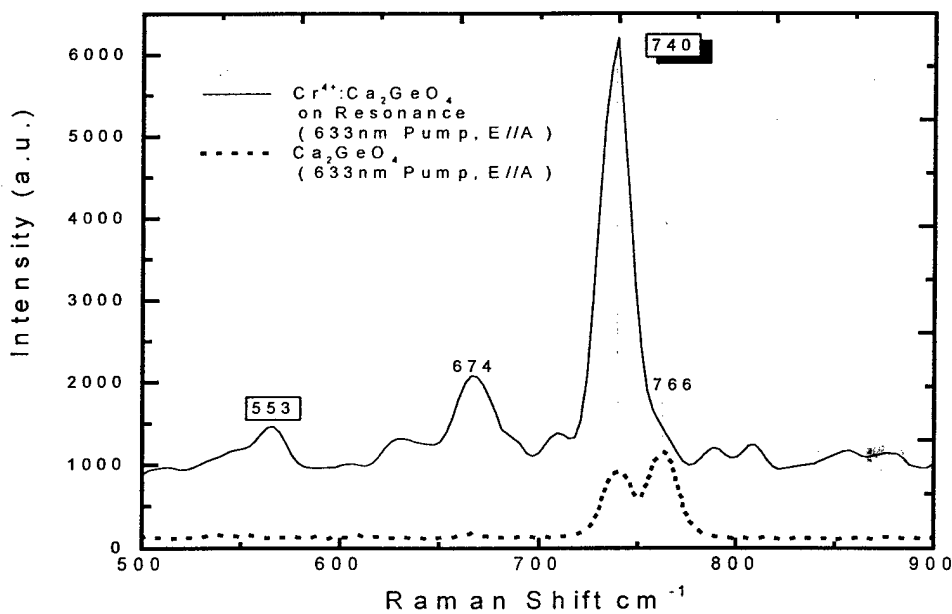


Fig.4 Resonance Raman spectrum (solid line) for doped Cr⁴⁺:Ca₂GeO₄ crystal and non-resonance Raman spectrum for undoped Ca₂GeO₄ crystal (dot line) in 500–900 cm⁻¹ with 633 nm pump. Both excitation and detection polarization directions were parallel to the “a” axis (E || a).

absorb a second photon to reach an excitation level. Up-converted hot luminescence spectra obtained under different laser wavelengths are shown in Fig. 5. The lower profile was obtained under 598 nm (2.073 eV) laser excitation, which photoexcites Cr^{4+} ions to $E_{\text{EL}} = 3.116 \pm 0.001$ eV (i.e., 2.073 eV above the metastable level). The upper profile was obtained under 588 nm (2.108 eV) laser excitation, which photoexcites Cr^{4+} ions to $E_{\text{EL}} = 3.151 \pm 0.001$ eV (i.e., 2.108 eV above the metastable level). In both cases, three main peaks appear with the highest energy peak, positioned at E_{EL} . The salient feature displayed in Fig. 5 is the location of the secondary peaks. The secondary peaks show the energy of the phonon modes involved in the initial steps of the nonradiative relaxation, given by the energy difference between successive peaks. The measured energy of these modes in both cases is at energy $E_{\text{phonon}} = 726 \pm 25$ cm^{-1} . The energy of the phonons involved in the initial steps of the nonradiative relaxation ($E_{\text{phonon}} = 726 \pm 25$ cm^{-1}) in $\text{Cr}^{4+}:\text{Ca}_2\text{GeO}_4$ coincides with the energy of the only phonon mode (located at 733 cm^{-1}) in resonance with a local mode of the relaxing impurity ion. The primary step in the nonradiative relaxation process is $\omega_L \rightarrow \omega_P$. Thus energy resonance between local and phonon modes is a key criterion in selecting the phonon modes that participate in the nonradiative relaxation.

The initiation of the nonradiative decay process leads to complete draining of the energy stored in the metastable level of the impurity lasing ion. Consequently, the physics that governs the initial steps of this process is of great importance. In laser materials, it is desirable to minimize the nonradiative relaxation in order to obtain higher laser quantum efficiency and to reduce the power requirements and cost for the photoexcitation source of the laser medium. This work suggests that this can be achieved by reducing the number of effective decay channels, that is, the number of energy resonance phonon-local mode pairs. The simplest solution to this problem is to reduce the total number of phonon and local modes. The number of local modes depends on the number of neighboring ions of the impurity optically active ion, the size of the lattice ions, and interatomic forces. In the first approximation, only first neighbors are involved in the local vibrations. However, when the force constants are large, second neighbors also participate in the local vibrations, increasing the number of local modes. This is the case in forsterite,

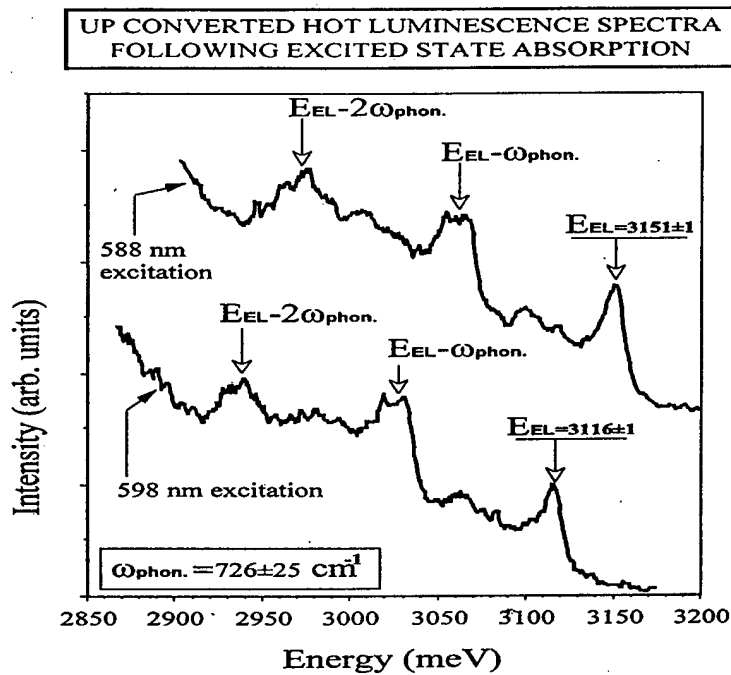


Fig. 5 Upconverted hot luminescence spectra following excited state absorption under 598 nm excitation (lower profile) and 588 nm excitation (upper profile) at liquid nitrogen temperature.

where the large number of local modes is due to the second neighbor interactions. The number of phonon modes depends on the total number of ions per unit cell; consequently, the possible number of in-resonance local-phonon modes pairs can be reduced by choosing a simple unit cell.